13th International Conference on Applications of Statistics and Probability in Civil Engineering, ICASP13
Seoul, South Korea, May 26-30, 2019

Selecting Representative Scenarios for Contingency Analysis of Infrastructure Systems with Dependent Component Failures

Hugo Rosero-Velásquez
PhD Student, Engineering Risk Analysis Group, Technische Universität München, Germany

Daniel Straub
Professor, Engineering Risk Analysis Group, Technische Universität München, Germany

ABSTRACT:

Classical contingency analysis assesses the robustness of infrastructure systems by removing one component at the time (sometimes up to two components) and evaluating the effect on the system performance Y. In systems with dependent component failures, this approach might not identify critical system failure scenarios, e.g. if failures are caused by natural hazards or other common causes. In this contribution, we develop an approach to identify representative scenarios S_T of component failures that are associated with damages or performance losses of a specific return period T. In practice, such scenarios are mostly defined based on historical data and expert knowledge, which often reflect past events but might not be representative of future events. Our approach is based on an initial Monte Carlo analysis of the system, resulting in an annual exceedance probability function of the system performance Y. Samples that approximately correspond to the value of Y associated with the return period of interest T are selected. The representative scenario for T is then identified by means of a clustering algorithm applied to these samples. The approach is demonstrated on a numerical example.

1. INTRODUCTION

Reliability of infrastructure networks, such as power grids, is often evaluated through contingency analyses, in which one or two components are assumed to fail. For a system with N components that might fail, there are at most $\frac{N(N-1)}{2}$ out of 2^N cases considered. An application for analyzing a power distribution system considering $N-1$ contingencies can be found in Acosta et al. (2018), while $N-2$ contingencies are compared with an influence-graph model in Hines et al. (2017). They are also studied for defining a risk-based ranking in Kengkla and Hoonchareon (2018). Additionally, a so-called $N-1-1$ contingency has been proposed, which considers a sequence of two failures (Mitra et al., 2016). This requires the analysis of $N(N-1)$ out of $N!$ cases.

As highlighted by Kengkla and Hoonchareon (2018), for complex reliable systems with large N and high redundancy, contingencies with more than two failed components should be considered for observing extreme black outs. $N-M$ contingencies have already been studied by Srivastava et al. (2018) in the context of attack scenarios, combining graph theory and DC power flow measures. In addition, Pescaroli and Alexander (2018) provides a framework for analyzing the impact of natural hazards to lifeline systems, while Scherb et al. (2017) develops a generic hazard model for being coupled with a system and ranking single components based on a network efficiency measure.

In a large system, there is a very large number of possible scenarios leading to some performance loss. For risk assessment and management pur-

poses, it is often convenient or even required to consider only a few representative loss scenarios. Typically, these are scenarios associated to a specific return period. Such representative scenarios can inform the contingencies to be analyzed in detail.

In this paper, we propose a methodology for selecting representative scenarios of component failures in an infrastructure system, based on the reliability of the system components, a performance measure and a return period of interest.

2. GENERIC INFRASTRUCTURE SYSTEM MODEL

We model a system with N components as a weighted graph with N_D nodes and N_E edges. A component can either be a node (e.g. a substation or a bus in a transmission grid) or an edge (e.g. transmission lines), thus $N = N_D + N_E$. Each edge has a weight, which for example represents the resistance in a transmission line or the pressure gradient in a pipeline. Moreover, the system shall have at least one source node and one terminal node.

Each component has a binary state X_i. During a hazard event, the reliability of the component is $p_i = \Pr(X_i = 1)$. The complete system is described by the component vector state $\mathbf{X} = (X_1, X_2, ..., X_N)$, which takes 2^N possible values. The probability associated to each state is a function of the marginal component reliabilities and the dependence between component states.

The component vector state $\mathbf{X}$ is mapped to the system performance measure Y (e.g. power loss) by means of a system model g (see Straub, 2018) :

$$Y = g(\mathbf{X}) \tag{1}$$

In the following, Y represents a loss of performance relative to the fully functioning system.

The system model g can be deterministic or stochastic. In most systems, it should consider cascading effects, caused by a redistribution of loads in the system following initial component failures. Cascading failure models are described in the literature (e.g., Crucitti et al., 2004; Hernández-Fajardo and Dueñas-Osorio, 2013; Scherb et al., 2017).

The system loss Y is a random variable, with exceedance probability (EP) function $H_Y(y) = \Pr(Y > y)$. Since Y is the loss of the system following a hazard event, this EP function is related to the annual exceedance rate AER through

$$AER(y) = \lambda_H H_Y(y) \tag{2}$$

with λ_H representing the annual frequency of the hazard occurrence. It follows that the loss with return period T is

$$Y_T = H_Y^{-1}\left(\frac{1}{\lambda_H T}\right) \tag{3}$$

Based on the above, a scenario S is defined as the tuple $(\mathbf{x}, y)$, where $\mathbf{x}, y$ are realizations of the random variables $\mathbf{X}, Y$. A representative scenario S_T associated to a return period T is a scenario which in some sense is representative of all scenarios within a range $\frac{1}{T}(1 \pm \Delta)$.

3. METHODOLOGY

In this Section we introduce a methodology for identifying the representative scenarios S_T. It hinges upon the availability of a computationally sufficiently cheap system model g, such that a crude Monte Carlo simulation (MCS) with around $10T\lambda_H$ samples can be performed. Many network system models used in the literature fullfill this criterion, (e.g., Shinozuka et al., 1999; Poljanšek et al., 2011; Hernández-Fajardo and Dueñas-Osorio, 2013). If a more expensive model is available and preferable, the methodology might nevertheless be applied on a cheaper (surrogate) model. The identified scenarios S_T can then be evaluated with the expensive model to evaluate the risk.

The first step is to perform a MCS, where n_s samples of $\mathbf{X}$ are generated. The minimum number of samples n_s should be selected in function of the maximum return period of interest T_{max}, such that $n_s > 10T_{max}\lambda_H$.

Samples of the component vector state $\mathbf{x}_1, \mathbf{x}_2, ..., \mathbf{x}_{n_s}$ are generated and the model $g(\mathbf{x}_k)$ is evaluated for each sample k, resulting in samples of system performance $y_1, ..., y_{n_s}$. The EP function $H_Y(y)$ is then constructed empirically as the complement of the sample CDF. Based on this function, one can associate to each $y_1, ..., y_{n_s}$ a corresponding return period $\hat{T}_1, ..., \hat{T}_{n_s}$ by means of Equation (3).

The second step is to associate sample tuples $(\mathbf{x}_k, y_k)$ to a return period of interest T. To this end, one defines an interval $\Omega_{T,\Delta} = \left[\frac{1}{T}(1-\Delta), \frac{1}{T}(1+\Delta)\right)$, with the parameter $\Delta > 0$ specifying the width of the interval. All sample tuples $(\mathbf{x}_k, y_k)$ whose corresponding $\frac{1}{\hat{T}_k}$ falls into this interval are collected. Note that the interval is symmetric around T in terms of exceedance probability. This ensures that the expected exeedance probability of all samples in the interval is $\frac{1}{T}$.

The choice of Δ must balance the accuracy and robustness of the selected scenarios. A small Δ leads to a high accuracy in the scenario return period, but implies that a smaller number of samples falls into $\Omega_{T,\Delta}$. Hence the identified scenario may be less robust. In contrast, a larger Δ causes scenarios with return periods different than T to be included in the interval. As a consequence, the selected scenario S_T can be associated with a return period that differs more from T.

Since the number of samples that fall into the interval decrease with increasing T for a fixed Δ, it can be optimal to vary Δ with T. For example, one can select Δ by fixing the expected number of samples n_v in $\Omega_{T,\Delta}$, which approximates the probability of one sample to fall into that interval:

$$\Pr\left(\frac{1}{\lambda_H \hat{T}_i} \in \Omega_{T,\Delta}\right) \approx \frac{n_v}{n_s} \tag{4}$$

Solving for Δ results in:

$$\Delta \approx \frac{\lambda_H T n_v}{2 n_s} \tag{5}$$

The third step is to identify a representative $\mathbf{x}$ among the collected samples in $\Omega_{T,\Delta}$. A clustering algorithm is applied to these samples. If there is a cluster whose size is significantly larger, then the tuple $(\mathbf{x}, y)$ corresponding to the mode of that cluster is selected as the representative scenario S_T.

In most cases, multiple return periods $T_1, T_2, ..., T_q = T_{max}$ are of interest. In this case, steps 2 and 3 are repeated for each $T = T_j$.

3.1. Clustering algorithm

Among the available clustering algorithms, we utilize DBSCAN (see Ester et al., 1996) for identifying the representative scenarios. DBSCAN determines the clusters based on the parameter ε, the maximum distance between points in a cluster, and the parameter k, the minimum number of points for a subset to become a cluster. These two parameters determine whether two points are density reachable, i.e. whether they are part of non-disjoint neighborhoods of radius ε, each of them containing at least k points. Finally, clusters are determined as the non-empty maximal subsets of points that are density connected with respect to ε and k. Some samples do not belong to any cluster, these are labeled as noise. Importantly, DBSCAN does not require one to predefine the number of clusters.

The choice of k determines the minimum size of any cluster. In cases where there are few repeated samples, there is a higher chance that the largest cluster has a size close to k. If k is small, then the algorithm is likely to result in multiple small clusters, while a large k increases the fraction of samples labeled as noise.

Ester et al. (1996) suggest to choose ε and k according to the EP function of the distances of each point to their k-nearest neighbor. That function provides an indication on the expected percentage of samples labelled as noise for a given combination of ε and k. In the context of the considered application, we suggest to fix k and then determine ε based on this EP function. By increasing ε, the small clusters are merged and some samples, formerly classified as noise, might now be added to the new clusters. However, an ε close to $\sqrt{N}$ classifies the n_v samples into one single cluster.

3.2. Example with a small system

For illustrating the methodology, we consider a small system with $N = 10$ components, whose performance is measured by the following weighted sum:

$$g(\mathbf{x}) = \frac{2}{N(N+1)} \sum_{i=1}^{N} i(1-x_i) \tag{6}$$

That is $0 \leq g(\mathbf{x}) \leq 1$. The performance function is evaluated through a MCS with sample size of $n_s = 2 \times 10^4$.

The component failure probability follows a beta distribution with mean $p_i = p = 0.99$ and standard deviation $\sigma_p = 0.05$. Thus the number of available components N_a follows a beta-binomial distri-

bution, whose probability mass function is:

$$Pr(N_a = n) = \binom{N}{n} \frac{B(n+r, N-n+s)}{B(r,s)} \quad (7)$$

The beta-binomial distribution introduces a dependence among the components, which is defined by σ_p. If $\sigma_p = 0$, the components fail independently, while $\sigma_p = \sqrt{p(1-p)}$ implies that either none or all components fail, the latter event with probability $1-p$. Therefore, it is convenient to describe the dependence between the components by the normalized measure $\gamma_p = \frac{\sigma_p}{\sqrt{p(1-p)}}$ (Straub, 2018).

Figure 1 shows the EP function obtained from the n_s samples. The dashed lines bound the intervals $\Omega_{T,\Delta}$. We consider two return periods of interest ($T_1 = 10^2$ and $T_2 = 10^3$ years) and $\lambda_H = 1.0\text{yr}^{-1}$. Based on Equation (5), for the return period of 10^2 years, we found that $\Delta = 0.1$ results in an expected number of 200 samples, while for 10^3 years we expect 100 samples with $\Delta = 0.5$. The resulting sample size for each interval for the specific MCS is 241 samples for 10^2 years and 105 for 10^3 years.

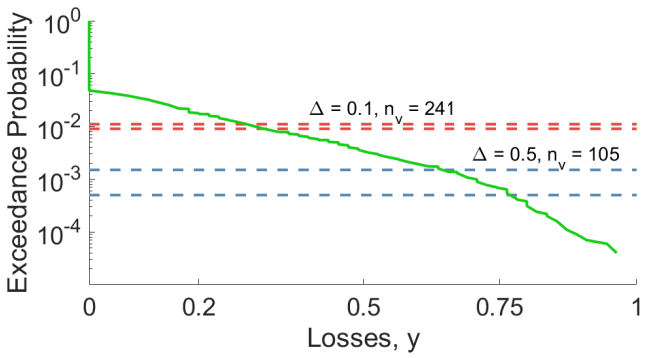

Figure 1: System EP function, with the intervals $\Omega_{T,\Delta}$ for return periods of $T = 10^2$ years (red) and $T = 10^3$ years (blue).

The samples of the MCS are displayed in Figure 2, located according to the vertices of the unit 10-hypercube graph. The hypercube projection arranges the vertices in such way that each column groups the vertices with the same number of failed components. Since every edge in an unit hypercube has length one, such a projection has the property that the edges only connect nodes located in different but adjacent columns.

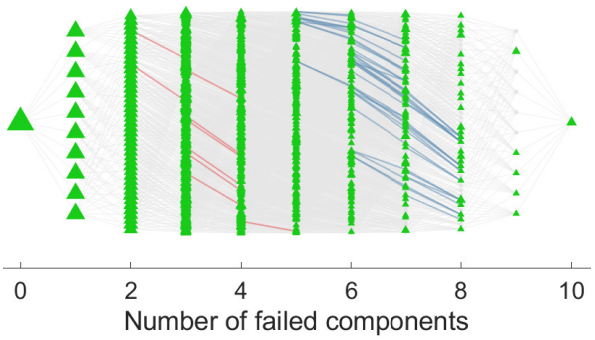

Figure 2: Sample of vector states located on the projection of a 10-hypercube, with vertices arranged by number of failed components. Sample sets for return periods of $T = 10^2$ years (red) and $T = 10^3$ years (blue) are highlighted, and the marker size is proportional to the frequency of each state in the samples.

As one can see from Figure 1, the state without failed components is the most frequent one, representing more than 90% of the samples. Accordingly, it is the largest vertex of the hypercube in Figure 2, which also shows that the frequency of each state decreases with the number of failed components.

The result of applying the DBSCAN algorithm to the highlighted sample subsets is shown in Figure 3, for selected values of ε and k. With $\varepsilon \geq \sqrt{2}$, all samples are assigned to the same cluster, which is consequence of the small number of components in this example. Therefore, we recommend to fix $\varepsilon = 1$ for systems with few components and high component reliability. In contrast, in systems with many components, a larger ε can be a reasonable choice. In such case, the EP function of the k-distances gets smoother, and the expected percentage of noise can be controlled by following the procedure of Ester et al. (1996).

From Figure 3, one can also observe that the increase of parameter k increases the percentage of samples labelled as noise. This becomes critical for large return periods, where Δ is larger and the samples to be clustered are more sparse in the hypercube. For this set of samples, increasing k from 4 to 6 increases the the percentage of noise from 9% to 23% for a return period of 10^2 years, and from 27% to 67% for a return period of 10^3 years. However, the sample size is sufficiently large that the mode

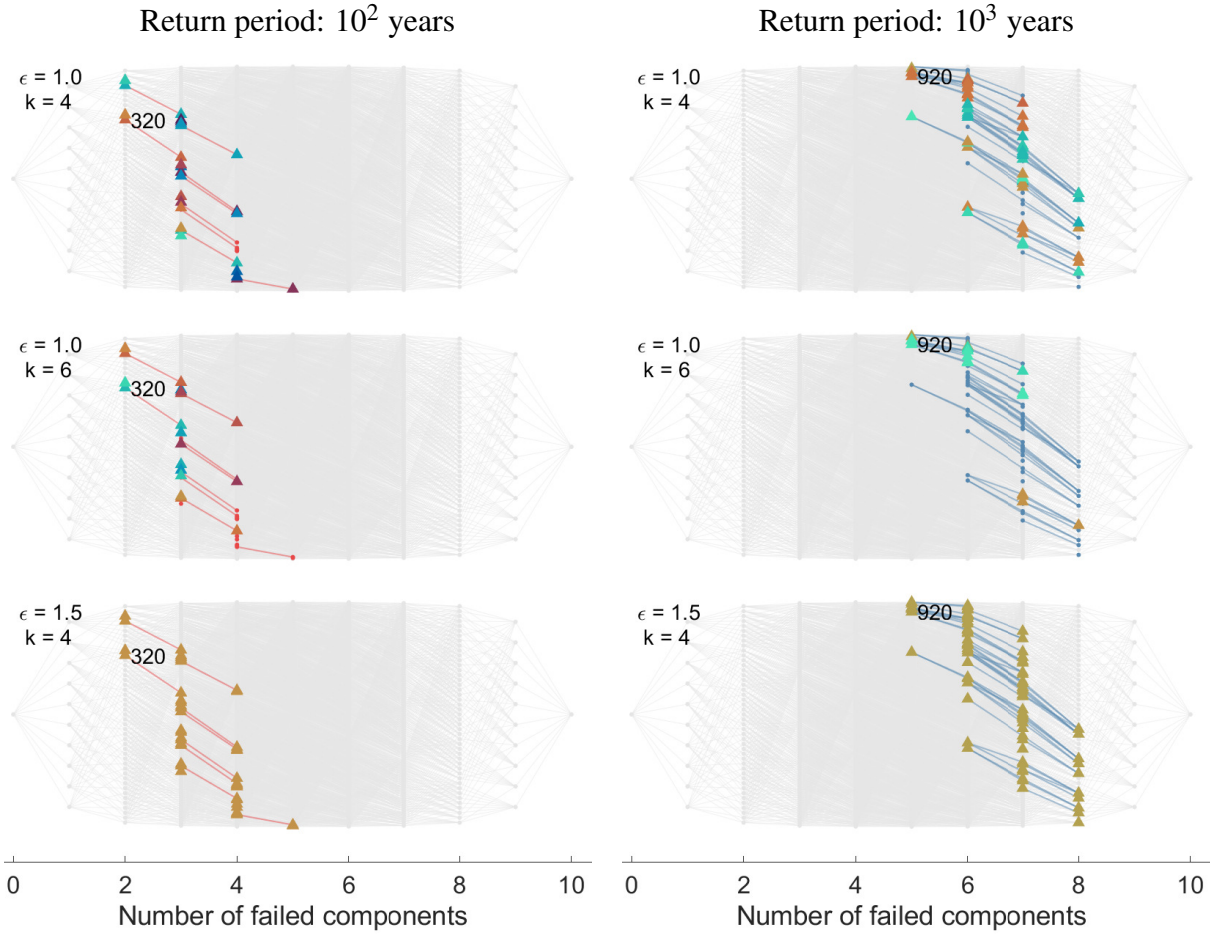

Figure 3: Clustered vector states for return periods of 10^2 *and* 10^3 *years and the labels of their representative scenarios. The dots correspond to states classified as noise. The number label indicates the representative scenario for each interval, whose binary representation tells which are the components that fail, e.g. state* 2^{j-1} *corresponds to the single failure of the j-th component, for* $j = 1,...,N$.

of the largest cluster does not change with variation of ε and k, which indicates the robustness of the representative scenario.

4. Application to an electric grid

We apply the methodology to the IEEE39 bus system, whose topology is displayed in Figure 4. It consists of 39 nodes and 43 edges. The edge weights correspond to the line reactance values; the line capacities are here modeled as being proportional to the number of shortest paths passing through them. This example was previously studied by Scherb et al. (2017) for quantifying the network reliability considering cascading effects and exposure to spatially distributed hazards.

The system performance is evaluated by the efficiency loss:

$$g(\mathbf{x}) = 1 - \frac{E(\mathbf{x})}{E(\mathbf{1})} \tag{8}$$

$$E(\mathbf{x}) = \frac{1}{|SN||TN|} \sum_{\substack{s \in SN \\ t \in TN \\ s \neq t}} \text{eff}_{st} \tag{9}$$

where eff_{st} is the efficiency of the most efficient path from source node s to terminal node t, SN is the set of source nodes, TN the set of terminal nodes. $E(\mathbf{x})$ is the network efficiency associated to the component vector state $\mathbf{x}$ and $E(\mathbf{1})$ is the efficiency of the intact system. The efficiency of a path

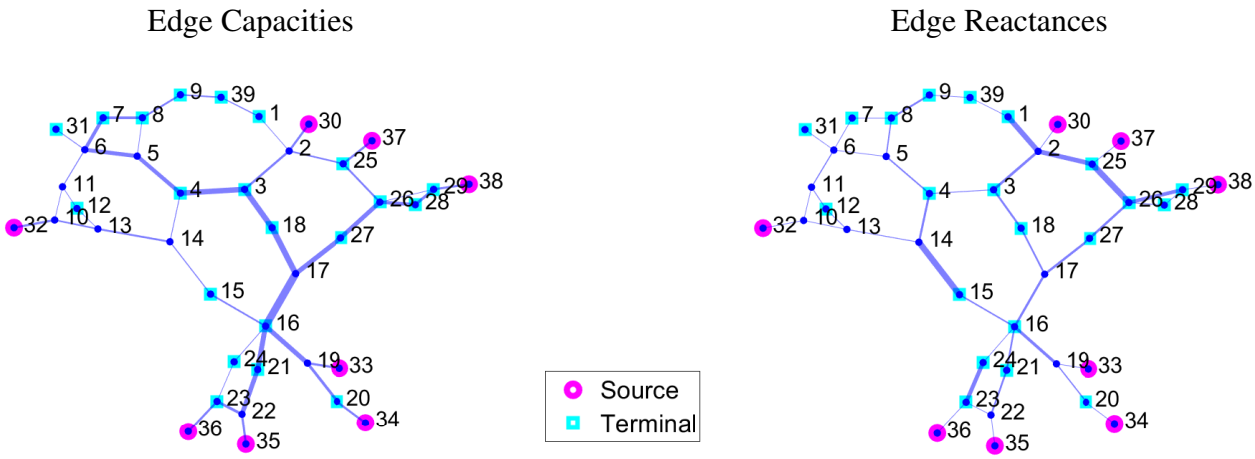

Figure 4: IEEE39 bus system, with edge thicknesses proportional to their estimated capacities (left) and reactances (right).

is equal to the sum of the reactance values along that path. Equation (9) is a modified version of the network efficiency defined by Latora and Marchiori (2001), restricted to paths that connect nodes from SN to nodes in TN. Equation (8) is the compliment of the network efficiency defined by Scherb et al. (2017).

In this example, two types of dependencies are considered: Initial failures at nodes and line failures by cascading effects. The first one is modelled by the beta-binomial distribution with different values of γ_p following Section 3.2. The cascading effects are evaluated with the efficiency-based model proposed by Crucitti et al. (2004) and later extended by Hernández-Fajardo and Dueñas-Osorio (2013) and Scherb et al. (2017). This model of cascading effects is deterministic, i.e. for a given set of initially failed nodes, there is only one possible final state of the system.

For the performance loss, the return period of interest is 10^2 years. The generic hazard has frequency $\lambda_H = 1.0\text{yr}^{-1}$. The marginal component probability of failure during a hazard event is 0.01. A MCS is performed with sample size $n_s = 5 \times 10^5$.

4.1. EP function for different γ_p

Figure 5 shows the EP functions for dependency measure $\gamma_p = 0.0, 0.2, 0.5$ and 0.7. One can observe the transition from the case of independent initial failures, where scenarios of high losses are rare and initial failures of few nodes are most likely, to the limit case of fully dependent components ($\gamma_p = 1.0$), in which the system performance following a hazard event corresponds to a Bernoulli random variable with probability $\Pr(Y = 0|Hazard) = 0.01$.

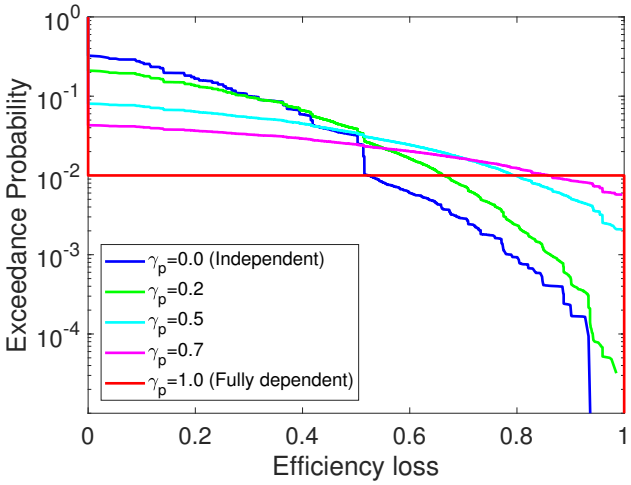

Figure 5: EP functions for different dependence measures γ_p and mean component reliability of $p = 0.99$

4.2. Clustering and representative scenarios

We find the representative scenario for the $T = 100$ year return period, by requiring a minimum number of samples $n_v = 10^3$ whose EP falls in $\Omega_{T,\Delta}$. According to Equation (5), this requires $\Delta = 0.1$. Since we apply the clustering algorithm to

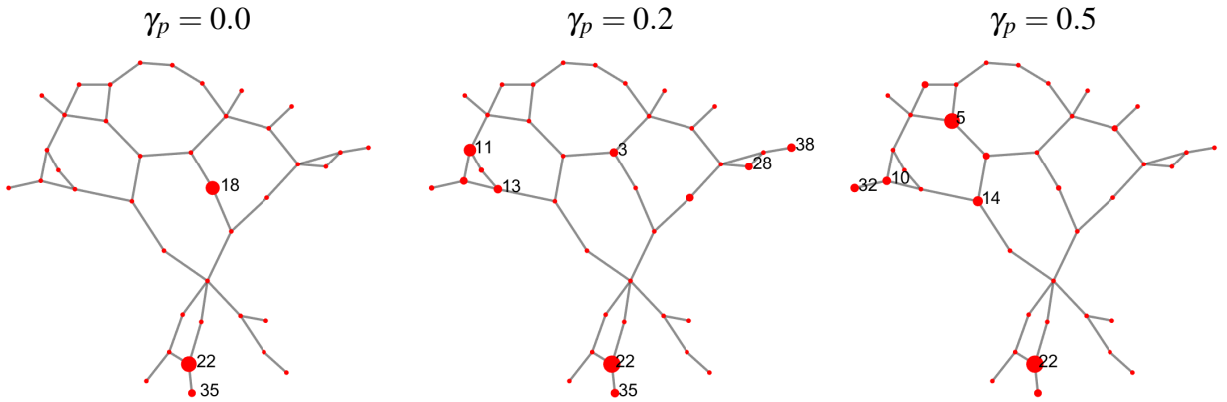

Cluster modes	Rel. freq.
22	0.47
18	0.40
35	0.13

Cluster modes	Rel. freq.
11,22	0.33
22,38	0.17
3,13	0.17
28,35	0.13

Cluster modes	Rel. freq.
14,22	0.23
5,10	0.17
5,32	0.17
5,22	0.13

Figure 6: Representative scenarios for return period of $T = 100$ years and different dependence measures γ_p based on 30 repeated analyses. The size of the markers is proportional to the relative frequency that failure of the node is part of a representative scenario among the 30 repetitions. The table summarizes the most frequent representative scenarios, together with their relative frequencies in the 30 repetitions.

the final states of the edges, the samples are vertices of the 43-hypercube graph.

For assessing the robustness of the scenario selection, we repeat the MCS and the subsequent analysis 30 times for each dependence measure γ_p. The results are summarized in Figure 6.

As evident from Figure 6, the identified representative scenarios can differ when repeating the analysis with different MCS samples. This effect is more severe with increasing dependence among component failures. Among 30 repetitions, in the case of $\gamma_p = 0$ we find three different representative scenarios, in the case of $\gamma_p = 0.2$ we find eight different representative scenarios, in case of $\gamma_p = 0.5$ we find nine different representative scenarios, and for $\gamma_p = 0.7$ we find 28 different representative scenarios. This effect might be related to the fact that the EP functions become flatter around $EP = 10^{-2}$ with increasing γ_p (see Figure 5). This indicates that the choice of the mode in the cluster as the representative scenario might not generally lead to robust choices.

5. CONCLUSIONS

We introduce a methodology for selecting representative scenarios of component failures in infrastructure systems, which can be utilized in contingency analyses and risk assessments. The scenarios are representative for a fixed return period of performance losses. The procedure is based on performing an initial Monte Carlo simulation, assuming a sufficiently cheap computational model of the system performance is available, and a cluster analysis to identify the representative combination of component failures. The application on two examples demonstrates the feasibility of the method, but highlights that selecting the representative scenario as the mode of the identified clusters may not always be a robust approach.

6. ACKNOWLEDGEMENTS

This work has been sponsored by the research and development project RIESGOS (Grant No. 03G0876), funded by the German Federal Ministry of Education and Research (BMBF) as part of the funding programme "BMBF CLIENT II – International Partnerships for Sustainable Innovations".

7. REFERENCES

Acosta, J. S., López, J. C., and Rider, M. J. (2018). "Optimal multi-scenario, multi-objective allocation of fault indicators in electrical distribution systems using a mixed-integer linear programming model." *IEEE Transactions on Smart Grid (early access)*, 1–1.

Crucitti, P., Latora, V., and Marchiori, M. (2004). "Model for cascading failures in complex networks." *Phys. Rev. E*, 69, 045104.

Ester, M., Kriegel, H.-P., Sander, J., and Xu, X. (1996). "A density-based algorithm for discovering clusters a density-based algorithm for discovering clusters in large spatial databases with noise." *KDD'96 Conference Proceedings*, AAAI Press, 226–231.

Hernández-Fajardo, I. and Dueñas-Osorio, L. (2013). "Probabilistic study of cascading failures in complex interdependent lifeline systems." *Reliability Engineering System Safety*, 111, 260–272.

Hines, P., Dobson, I., and Rezaei, P. (2017). "Cascading power outages propagate locally in an influence graph that is not the actual grid topology." *IEEE Transactions on Power Systems*, 32(2), 958–967.

Kengkla, N. and Hoonchareon, N. (2018). "Risk-based n-2 contingency ranking in transmission system using operational condition." *ICEAST Conference Proceedings*.

Latora, V. and Marchiori, M. (2001). "Efficient behavior of small-world networks." *Phys. Rev. Lett.*, 87, 198701–198701–4.

Mitra, P., Vittal, V., Keel, B., and Mistry, J. (2016). "A systematic approach to n-1-1 analysis for power system security assessment." *IEEE Power and Energy Technology Systems Journal*, 3(2), 71–80.

Pescaroli, G. and Alexander, D. (2018). "Understanding compound, interconnected, interacting, and cascading risks: A holistic framework." *Risk Anal.*, 38(11), 2245–2257.

Poljanšek, K., Bono, F., and Gutiérrez, E. (2011). "Seismic risk assessment of interdependent critical infrastructure systems: The case of european gas and electricity networks." *Earthquake Engineering and Structural Dynamics*, 41(1), 61–79.

Scherb, A., Garrè, L., and Straub, D. (2017). "Reliability and component importance in networks subject to spatially distributed hazards followed by cascading failures." *ASME J. Risk Uncertain. B*, 3(2), 021007.

Shinozuka, M., Cheng, T., and Feng, M. Q. (1999). "Seismic performance analysis of electric power systems." *MCEER Research Progress and Accomplishments 1997-1999*, 61–69.

Srivastava, A. K., Ernster, T. A., Liu, R., and Krishnan, V. G. (2018). "Graph-theoretic algorithms for cyber-physical vulnerability analysis of power grid with incomplete information." *Journal of Modern Power Systems and Clean Energy*, 6(5), 887–899.

Straub, D. (2018). *Lecture Notes in Engineering Risk Analysis*. ERA Group, Technische Universität München.